

- Fleischer, S., McIntyre, J. O., Stoffel, W., & Tungal, B. D. (1979) *Biochemistry* 18, 2420-2429.
- Godici, P. E., & Landsberger, F. R. (1974) *Biochemistry* 13, 362-368.
- Harina, B. M., Dyckes, D. F., Wilcott, M. R., III, & Jones, W. C., Jr. (1978) *J. Am. Chem. Soc.* 100, 4897-4899.
- Jones, W. C., Jr., Rothgeb, J. M., & Gurd, F. R. N. (1975) *J. Am. Chem. Soc.* 97, 3875-3877.
- Jones, W. C., Jr., Rothgeb, J. M., & Gurd, F. R. N. (1976) *J. Biol. Chem.* 251, 7452-7460.
- Keniry, M. A., & Smith, R. (1979) *Biochim. Biophys. Acta* 578, 381-391.
- Lee, A. G., Birdsall, N. J. M., & Metcalfe, J. C. (1974) *Methods Membr. Biol.* 2, 1-156.
- Levine, Y. K., Birdsall, N. J. M., Lee, A. G., & Metcalfe, J. C. (1972) *Biochemistry* 11, 1416-1421.
- Lowden, J. A., Moscarello, M. A., & Morecki, R. (1966) *Can. J. Biochem. Physiol.* 44, 567-577.
- Maugh, T. H. (1977) *Science* 195, 969-971.
- Moscarello, M. A. (1976) *Curr. Top. Membr. Transp.* 8, 1-28.
- Palmer, F. B., & Dawson, R. M. C. (1969) *Biochem. J.* 111, 629-636.
- Papahadjopoulos, D., & Miller, N. (1967) *Biochim. Biophys. Acta* 135, 624-638.
- Papahadjopoulos, D., Jacobson, K., Nir, S., & Isac, T. (1973) *Biochim. Biophys. Acta* 311, 330-348.
- Papahadjopoulos, D., Moscarello, M. A., Eylar, E. H., & Isac, T. (1975) *Biochim. Biophys. Acta* 401, 317-335.
- Schejter, A., Lanir, A., Vig, I., & Cohen, J. S. (1978) *J. Biol. Chem.* 253, 3768-3770.
- Smith, R. (1977) *Biochim. Biophys. Acta* 470, 170-184.

New Calcium Indicators and Buffers with High Selectivity against Magnesium and Protons: Design, Synthesis, and Properties of Prototype Structures[†]

Roger Y. Tsien

ABSTRACT: A new family of high-affinity buffers and optical indicators for Ca^{2+} is rationally designed and synthesized. The parent compound is 1,2-bis(*o*-aminophenoxy)ethane-*N,N,N',N'*-tetraacetic acid (BAPTA), a relative of the well-known chelator EGTA [ethylene glycol bis(β -aminoethyl ether)-*N,N,N',N'*-tetraacetic acid] in which methylene links between oxygen and nitrogen are replaced by benzene rings. BAPTA and its derivatives share the high ($>10^5$) selectivity for Ca^{2+} over Mg^{2+} of EGTA but are very much less affected by pH changes and are faster at taking up and releasing Ca^{2+} . The affinity of the parent compound for Ca^{2+} (dissociation constant 1.1×10^{-7} M in 0.1 M KCl) may be strengthened or weakened by electron-releasing or -withdrawing substituents on the

aromatic rings. The Ca^{2+} and Mg^{2+} affinities may further be altered by replacing the ether oxygens by heterocyclic nitrogen atoms. The compounds described are fluorescent Ca^{2+} indicators absorbing in the ultraviolet region; the very large spectral shifts observed on binding Ca^{2+} fit the prediction that complexation should hinder the conjugation of the nitrogen lone-pair electrons with the aromatic rings. Derivatives with quinoline nuclei are notable for their high sensitivity of fluorescent quantum yield to the binding of Ca^{2+} but not of Mg^{2+} . Preliminary biological tests have so far revealed little or no binding to membranes or toxic effects following intracellular microinjection.

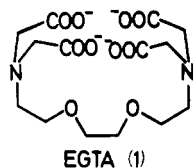
It is scarcely necessary any longer to stress the importance of intracellular free Ca^{2+} as a second messenger for external stimuli and as a regulatory ion. There is vast literature on this topic, and several recent symposia have been devoted to the cellular functions of Ca^{2+} (Duncan, 1976; Scarpa & Carafoli, 1978). A major technical challenge has been to devise satisfactory means for nondestructively measuring intracellular free Ca^{2+} with good time resolution [for reviews see Kretsinger & Nelson (1976) and Ashley & Campbell (1979)]. The most popular technique has been to use dyes or proteins which change their absorption or luminescence upon binding Ca^{2+} ions. In the past, these indicators have suffered from several problems (Brown et al., 1977; Thomas, 1979; Moisescu et al., 1975; Blinks et al., 1976, 1978): (1) insufficient selectivity against competing cations, particularly H^+ and Mg^{2+} ; (2) complex stoichiometries of interaction with Ca^{2+} , for example, 1 Ca^{2+} /2 dyes or several Ca^{2+} /1 protein; (3) inflexibility of

molecular design, or the difficulty of rationally adjusting indicator properties by tinkering with the molecular structure. This paper demonstrates that these problems can be largely overcome by new rational designs and chemical syntheses. The resulting simple compounds are both fluorescent indicators, absorbing in the ultraviolet region, and buffers with distinct advantages over previous buffers. Later papers will describe substantial progress toward the goal of superior visible Ca^{2+} indicators which can give fast quantitative readout of intracellular free Ca^{2+} concentrations in a wide variety of interesting physiological systems.

Consider EGTA¹ (ethylene glycol bis(β -aminoethyl ether)-*N,N,N',N'*-tetraacetic acid) (1). This compound is the only buffer with high selectivity for Ca^{2+} over Mg^{2+} to have found significant use in biological research. The $\text{Ca}^{2+}/\text{Mg}^{2+}$

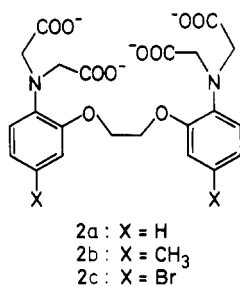
[†] From the Physiological Laboratory, University of Cambridge, Cambridge CB2 3EG, England. Received October 26, 1979. This work was supported by grants from the Science Research Council.

¹ Abbreviations used: EGTA, ethylene glycol bis(β -aminoethyl ether)-*N,N,N',N'*-tetraacetic acid; BAPTA, 1,2-bis(*o*-aminophenoxy)-ethane-*N,N,N',N'*-tetraacetic acid; Mops, 3-(*N*-morpholino)propane-sulfonic acid; Hepes, *N*-2-hydroxyethylpiperazine-*N'*-2-ethanesulfonic acid.



discrimination presumably stems from a binding cavity which has the right size for Ca^{2+} but which cannot constrict further to envelop Mg^{2+} snugly because the carboxyls at each end of the chain start butting into each other. Unfortunately, the nitrogens bind protons with pK_a s of 8.96 and 9.58 (Martell & Smith, 1974), making the Ca^{2+} -buffering level of EGTA strongly dependent on pH variations near 7. They also greatly slow down the uptake and release of Ca^{2+} . Hellam & Podolsky (1969) reported apparent forward and backward rate constants of $10^{6.3} \text{ M}^{-1} \text{ s}^{-1}$ and 0.4 s^{-1} for the reaction of Ca^{2+} with EGTA at pH 7.0, where EGTA exists predominately as the dianion $\text{H}_2\text{EGTA}^{2-}$. At physiological pH, EGTA binds Ca^{2+} 2 to 3 orders of magnitude more slowly than ligands without blocking protons and so takes up to seconds to buffer a Ca^{2+} transient.

How then could a suitable Ca^{2+} indicator be designed? It could be designed by hybridizing EGTA with some aromatic-ring chromophore, incorporating a large enveloping cavity with all the ligand pK_a s below 7 for speed and pH insensitivity. But how? After consideration of many alternatives, structure **2a** was designed. It can be seen as a derivative of EGTA in



which benzene rings replace the methylene groups connecting N to O with little effect on the overall geometry of the molecule. Therefore the cavity should be much the same desirable size and shape as EGTA but with the nitrogen pK_a s lowered from 8 or 9 down to 5 or 6. Furthermore, the UV spectrum of the compound could be predicted to change considerably between Ca^{2+} -free and Ca^{2+} -bound states. In the former, with no special constraint on the conformation of the molecule, the normal tendency of aromatic amine lone pairs to conjugate with rings would assert itself, so that the spectrum of an ordinary dialkylaniline or anisidine would be observed. However, in order for the nitrogens, their attached acetate groups, and the ether oxygens together to envelop and chelate a Ca^{2+} ion, the nitrogen-ring bonds would have to twist by nearly 90° , breaking the conjugation to the rings, giving a spectrum of a simple anisole or benzene.

Structure **2a** is provisionally named BAPTA as an acronym for bis(*o*-aminophenoxy)ethane-*N,N,N',N'*-tetraacetic acid. After it was synthesized and confirmed to have the predicted desirable properties, several more complex derivatives (**2b,c**, **3a,b**, **4**, and **5**) were prepared to explore the effect of molecular variations on optical properties and affinities for Ca^{2+} and Mg^{2+} .

Experimental Methods

^1H NMR peaks are presented in the following format: chemical shift on the τ scale; spin multiplicity (s = singlet, d = doublet, dd = doublet of doublets, t = triplet, q = quartet, m = complex multiplet, br = broad), with coupling constants

in hertz if appropriate; relative number of protons represented.

Synthesis of Ligands 2a-c. Sodium 2-nitrophenoxide [34.9 g (217 mmol)], 22.9 g (122 mmol) of 1,2-dibromoethane, and 50 mL of dimethylformamide were stirred and heated to 120°C under reflux. After 2 h the reaction mixture was cooled and the product filtered off and washed with more dimethylformamide, several portions of cold water, and ethanol. The yield was 18.6 g (56%) of faintly yellow crystals of 1,2-bis(2-nitrophenoxy)ethane: mp $168\text{--}169^\circ\text{C}$ [Jaunin & Holl (1958) reported $167.5\text{--}168^\circ\text{C}$]. This material was used directly in the next step. Further heating of the dimethylformamide filtrate gave a small additional yield of less pure material, which could be purified by recrystallization from hot 95% ethanol.

1,2-Bis(2-nitrophenoxy)ethane [10.2 g (33.5 mmol)], 215 mg of 10% palladium-on-charcoal catalyst, and 100 mL of 95% ethanol were hydrogenated at atmospheric pressure. Initially hydrogen was absorbed at 60 mL/min. After the mixture was shaken overnight, the total uptake was 4.715 L, 97.6% of the theoretical uptake. The ethanol was removed on a rotary evaporator, leaving 7.976 g of 1,2-bis(2-aminophenoxy)ethane (95% yield).

A 3.14-g sample of this material (containing 12.5 mmol of amine) was mixed with 13.4 g (62.6 mmol) of 1,8-bis(dimethylamino)naphthalene, 0.52 g (3.5 mmol) of anhydrous sodium iodide, 12.0 g (72 mmol) of ethyl bromoacetate, and 15 mL of acetonitrile (freshly distilled from phosphorus pentoxide). The mixture was stirred and heated to reflux under a nitrogen atmosphere for 20 h. After the mixture was cooled and diluted with toluene, the hydrogenation catalyst and precipitated bromide and iodide salts were filtered off and washed with more toluene. The combined organic phases were washed with several portions of phosphate buffer at pH 2, then washed with water, dried over MgSO_4 , and evaporated to give a residue of 6.77 g which crystallized as a brown mass. Recrystallization from ethanol yielded 5.2 g (71%) of 1,2-bis[2-[bis[(ethoxycarbonyl)methyl]amino]phenoxy]ethane (mp $95\text{--}97^\circ\text{C}$): NMR (CDCl_3 , 60 MHz) τ 3.09 (s, 8 H); 5.71 (s), 5.81 (s), 5.95 (q, 7 Hz) (total 20 H); 8.84 (t, 7 Hz, 12 H). This ester was saponified to the potassium salt of **2a** by dissolution in warm ethanol and addition of slightly more than 4 equiv of KOH as a concentrated aqueous solution. After the solution was gently warmed for about 30 min, the ethanol was evaporated in vacuo and the residue redissolved in water. The free acid could be obtained if desired by adding HCl to pH 2 and collecting, washing, and drying the resulting precipitate.

BAPTA (**2a**) can also be prepared by refluxing 1,2-bis(2-aminophenoxy)ethane with aqueous sodium chloroacetate with the pH maintained near 6 by intermittent addition of NaOH. This procedure seems more direct and uses cheaper reagents but proves more laborious and gives a less pure product than the ester route specified above. Also, the ester is preferred to the free acid for stability during long-term storage and as a building block for further syntheses.

The dimethyl analogue **2b** was prepared by saponification of its tetraethyl ester, synthesized by the previous route from 2-nitro-5-methylphenoxy in place of 2-nitrophenoxide. The ester had mp 120°C and NMR (CDCl_3 , 100 MHz) τ 3.08–3.38 (m, 6 H); 5.70 (s), 5.86 (s), 5.91 (q, 7 Hz) (total 20 H); 7.72 (s, 6 H); 8.82 (t, 7 Hz, 12 H).

The dibromo analogue **2c** was prepared from 1,2-bis[2-[bis[(ethoxycarbonyl)methyl]amino]phenoxy]ethane by dissolving 303 mg (0.52 mmol) in 5 mL of CHCl_3 (free from ethanol) plus 0.114 g (1.44 mmol) of pyridine. The mixture

was stirred and chilled in a liquid nitrogen-ethanol bath until the chloroform just began to freeze, whereupon 0.159 g (1.0 mmol) of Br₂ was added dropwise as a prechilled solution in CHCl₃. After the mixture was returned to room temperature, the solution was washed successively with dilute HCl, water, dilute aqueous NaHCO₃, and water, then dried over Na₂SO₄, and evaporated. The crude product formed in quantitative yield was recrystallized from diisopropyl ether to give 180 mg (47%) of 1,2-bis[2-[bis[(ethoxycarbonyl)methyl]amino]-5-bromophenoxy]ethane (mp 125–127 °C; NMR (CD₂Cl₂, 100 MHz) τ 2.69–3.1 (m, 4 H); 3.32 (d, 9 Hz, 2 H); 5.74 (s), 5.92 (s), 5.94 (q, 7 Hz) (total 20 H); 8.79 (t, 7 Hz, 12 H). This ester was hydrolyzed with KOH to the tetraanion **2c** as described above.

Synthesis of Ligand 3a. 2-Methyl-8-nitroquinoline [2.062 g (11.0 mmol)] (Madeja, 1962) and 0.743 g (9.1 mmol) of anhydrous sodium acetate were dissolved in 25 mL of hot acetic acid. The solution was cooled rapidly to room temperature, and 1.42 g (5.59 mmol) of iodine and 0.40 g (2.02 mmol) of sodium iodate were added with continual stirring. The iodate served to destroy iodide ions which would otherwise sequester the starting quinaldine as an insoluble triiodide complex. After the solution was stirred overnight at 25 °C, the light yellow precipitate of 2-(iodomethyl)-8-nitroquinoline was filtered off, washed with a little acetic acid, and dried; the yield was 73%. The acetic acid filtrate was neutralized with aqueous Na₂CO₃ and extracted with CH₂Cl₂. The organic phase was washed successively with aqueous Na₂CO₃, Na₂S₂O₃, H₂O, and saturated NaCl, dried over MgSO₄, and evaporated in vacuo to yield an additional 10% yield of the product: NMR (CDCl₃, 100 MHz) τ 1.8–2.4 (m, 5 H), 5.35 (s, 2 H).

Powdered 2-(iodomethyl)-8-nitroquinoline [2.47 g (7.84 mmol)] was added with stirring to a solution of 1.64 g (8.57 mmol) of potassium 2-nitro-5-methylphenoxide in 10 mL of dry dimethylformamide. The mixture soon crystallized but was then warmed briefly on a water bath to redissolve the crystals and ensure complete reaction. The cooled mixture was diluted with water. The resulting precipitate was filtered off, washed with aqueous sodium carbonate followed by distilled water, and then dried in vacuo. The crude yield was 2.43 g (91%). Recrystallization from chloroform yielded white crystals of 2-[(2-nitro-5-methylphenoxy)methyl]-8-nitroquinoline: 1.75 g, 66% yield; mp 189–190 °C; NMR (CDCl₃, 100 MHz) τ 1.6–3.2 (m, 8 H), 5.50 (s, 2 H), 7.67 (s, 3 H).

2-[(2-Nitro-5-methylphenoxy)methyl]-8-nitroquinoline [1.39 g (4.11 mmol)] as a slurry in 50 mL of ethanol was hydrogenated at atmospheric pressure with 260 mg of a 5% platinum-on-carbon catalyst preequilibrated with H₂. The platinum catalyst cannot be replaced by palladium, since palladium causes hydrogenolysis of the –CH₂–O– linkage at a rate competitive with nitro reduction. After 140 min of shaking, the uptake of hydrogen gas reached 99% of the theoretical volume. The greenish gray precipitate, containing product and charcoal catalyst, was filtered off. Recrystallization from chloroform-petroleum ether gave 0.78 g of bright yellow crystals of 2-[(2-amino-5-methylphenoxy)methyl]-8-aminoquinoline (68%). A further quantity of less pure material (11%) could be recovered from the initial ethanol filtrate by evaporation: NMR (CDCl₃, 100 MHz) τ 1.94 (d, 8.5 Hz, 1 H), 2.43 (d, 8.5 Hz, 1 H), 2.68 (dd, 7 and 8 Hz, 1 H), 2.87 (dd, 8 and 1.5 Hz, 1 H), 3.08 (dd, 7 and 1.5 Hz, 1 H), 3.27 (d, 1.5 Hz, 1 H), 3.35 (s, 1 H), 3.36 (d, 1.5 Hz, 1 H), 4.5–6.4 (br s, exchangeable with D₂O, 4 H), 4.64 (s, 2 H), 7.78 (s, 3 H).

2-[(2-Amino-5-methylphenoxy)methyl]-8-aminoquinoline [0.968 g (3.47 mmol)], 4.24 g (19.9 mmol) of 1,8-bis(dimethylamino)naphthalene, 3.34 g (20.0 mmol) of ethyl bromoacetate, 0.172 g (1.15 mmol) of anhydrous sodium iodide, and 10 mL of dry acetonitrile were refluxed under nitrogen with stirring. Further additions of 2.05 g (9.60 mmol) of 1,8-bis(dimethylamino)naphthalene and 3.27 g (19.6 mmol) of ethyl bromoacetate were made after the first 18 h. After a 66-h reflux, the mixture was cooled and diluted with toluene. The precipitate was filtered off and washed with fresh toluene. The combined filtrates were thoroughly washed with pH 2 phosphate buffer, then washed with distilled water, dried over magnesium sulfate, and evaporated in vacuo. The gummy yellow residue was chromatographed on silica gel with 2% (v/v) methanol in chloroform. The yield of 2-[[2-[bis[(ethoxycarbonyl)methyl]amino]-5-methylphenoxy]methyl]-8-[[bis[(ethoxycarbonyl)methyl]amino]quinoline was 73% (mp 63 °C): NMR (CDCl₃, 100 MHz) τ 1.95 (d, 8 Hz, 1 H); 2.38 (d, 8 Hz, 1 H); 2.6–2.85 (m, 2 H); 3.0–3.2 (m, 4 H); 4.75 (s, 2 H); 5.52 (s), 5.72 (q, 7 Hz), 5.80 (s), 5.90 (q, 7 Hz) (total 16 H); 7.78 (s, 3 H); 8.70 (t, 7 Hz), 8.80 (t, 7 Hz) (total 12 H). This tetraester was saponified as above with aqueous ethanolic KOH to give the tetrapotassium salt of compound **3a**.

Synthesis of Ligand 3b. 2-Methyl-6-methoxy-8-nitroquinoline [1.38 g (6.38 mmol)] (Mathur & Robinson, 1934), 0.244 g (2.98 mmol) of anhydrous sodium acetate, 0.270 g (1.36 mmol) of sodium iodate, 0.695 g (2.74 mmol) of iodine, and 6 mL of glacial acetic acid were stirred at room temperature overnight in the dark. The precipitate was filtered off, washed with acetic acid, and dried in vacuo, giving a 91% yield of 2-(iodomethyl)-6-methoxy-8-nitroquinoline as an orange solid sufficiently pure for the next step: NMR (CDCl₃, 80 MHz) τ 1.98 (d, 8.6 Hz, 1 H), 2.37 (d, ~3 Hz, 1 H), 2.45 (d, 8.7 Hz, 1 H), 2.81 (d, 3 Hz, 1 H), 5.41 (s, 2 H), 6.07 (s, 3 H).

A 1.98-g (5.75-mmol) sample of this iodo compound was treated with a solution of 1.91 g (10 mmol) of potassium 2-nitro-5-methylphenoxide in 15–20 mL of warm dimethylformamide. After 5 min of stirring at 75 °C, the mixture was cooled and diluted with 40 mL of water. The precipitate was collected, washed successively with aqueous sodium carbonate and water, and dried in vacuo, yielding 1.767 g (83%) of crude 2-[(2-nitro-5-methylphenoxy)methyl]-6-methoxy-8-nitroquinoline. Recrystallization from hot chloroform gave 1.31 g of yellow crystals (62% yield): mp 199–200 °C; NMR (CD₃COCD₃, 80 MHz) τ 1.51 (d, 8.8 Hz, 1 H), 2.07 (d, 8.8 Hz, 1 H), 2.15 (d, 3 Hz, 1 H), 2.18 (d, ~7 Hz, 1 H), 2.32 (d, 2.5 Hz, 1 H), 2.59 (s, 1 H), 3.03 (d, 7.4 Hz, 1 H), 4.51 (s, 2 H), 5.95 (s, 3 H), 7.56 (s, 3 H).

A 1.31-g (3.55-mmol) sample of this nitro compound was hydrogenated at 20 °C and 1 atm with 195 mg of 5% platinum-on-charcoal catalyst until 6 mol of hydrogen per mol of substrate was absorbed. The product, 2-[(2-amino-5-methylphenoxy)methyl]-6-methoxy-8-aminoquinoline, was filtered off, dried, and recrystallized from dichloromethane-petroleum ether (71% yield): mp 132–134 °C; NMR (CDCl₃, 100 MHz) τ 2.10 (d, 8 Hz, 1 H), 2.52 (d, 8 Hz, 1 H), 3.28 and 3.38 (3 H), 3.44 (d, 2.5 Hz, 1 H), 3.56 (d, 2.5 Hz, 1 H), 4.72 (s, 2 H), 5.70 (br s, 4 H, exchangeable with D₂O), 6.17 (s, 3 H), 7.80 (s, 3 H).

The preceding amine was alkylated with ethyl bromoacetate by the method described above. The viscous residue left after evaporation of toluene was crystallized by trituration with diisopropyl ether. The yield of 2-[[2-[bis[(ethoxycarbonyl)-

methyl]amino]-5-methylphenoxy]methyl]-6-methoxy-8-[bis-[(ethoxycarbonyl)methyl]amino]quinoline was 63%: mp 96–100 °C; NMR (CDCl₃, 80 MHz) τ 2.02 (d, 8.2 Hz, 1 H), 2.41 (d, 8.1 Hz, 1 H), 3.2–3.5 (m, 5 H), 4.75 (s, 2 H), 5.5–6.3 (m, 16 H), 7.83 (s, 3 H), 8.76 and 8.85 (overlapping triplets, 7 Hz, 12 H).

This ester was hydrolyzed with a slight excess of potassium hydroxide in warm ethanol. The solution was evaporated, and the residue, the potassium salt of ligand **3b**, was redissolved in D₂O: NMR (D₂O, 80 MHz) τ 1.89 (d, 8.5 Hz, 1 H), 2.49 (d, 8.5 Hz, 1 H), 3.1–3.4 (m, 5 H), 4.69 (s, 2 H), 5.82 (s, 4 H), 6.15 (s, 4 H + 3 H), 7.82 (s, 3 H).

Synthesis of Ligands 4–6. Ligand **4**, 1,2-bis[*N*-[2-[bis-(carboxymethyl)amino]phenyl]-*N*-(carboxymethyl)amino]-ethane, was prepared from 1,2-bis[(2-aminophenyl)amino]ethane (Tasker & Fleischer, 1970) by the usual alkylation with ethyl bromoacetate followed by saponification. Ligand **5**, 2-[[2-[bis(carboxymethyl)amino]-5-methylphenoxy]-methyl]-2,3-dihydro-7-[bis(carboxymethyl)amino]benzofuran, was prepared from 2-allyl-6-nitrophenol (Claisen & Eisleb, 1913) by bromination, ring closure to give 2-(bromo-methyl)-2,3-dihydro-7-nitrobenzofuran, reaction of this with potassium 2-nitro-5-methylphenoxide, catalytic hydrogenation, alkylation with ethyl bromoacetate, and saponification. Ligand **6**, 8-[bis(carboxymethyl)amino]quinoline, was prepared by alkylating 8-aminoquinoline with ethyl bromoacetate followed by saponification.

NMR spectra at 60 and 100 MHz were recorded on Varian EM-360 and HA-100 instruments locked on internal tetramethylsilane (or *tert*-butyl alcohol for D₂O spectra). Spectra at 80 MHz were obtained on a Varian CFT-20 Fourier transform machine using a deuterium lock. All spectra were run at 25–30 °C; spectra of the BAPTA tetraanion were obtained with sufficient K₂CO₃ in the D₂O to ensure complete ionization, the estimated pD being about 10.

Proton ionization constants were determined by suspending the free acid at 1 mmol/L in 0.1 M KCl at 20 °C and titrating with 0.1 M KOH. The titration curve was analyzed by a nonlinear least-squares fit to the standard equations for multiple ionizations (Beck, 1970).

UV absorption spectra were recorded on a Pye Unicam SP800 dual-beam spectrophotometer at 22 ± 2 °C. When more precise absorbance readings were required, as in the determination of the affinity of BAPTA for Ca²⁺, samples were also measured on a Zeiss PMQII single-beam instrument.

Free [Ca²⁺] levels below 1 μ M were controlled by Ca-EGTA buffers in 0.1 M KCl, assuming an apparent log stability constant for Ca-EGTA of 7.00 at pH 7.29. This value is calculated from the data of Martell & Smith (1974) using the recommended correction (+0.11) for the proton ionization constants of EGTA. Detailed compositions of the buffers are listed in the figure legends. Free [Ca²⁺] levels between 1 and 10 μ M were maintained by analogous Ca²⁺ buffers based on *N*-(hydroxyethyl)ethylenediamine-*N,N',N'*-triacetic acid.

Free [Mg²⁺] was likewise controlled by Mg-EGTA buffers assuming an apparent dissociation constant for Mg-EGTA + Mg-HEGTA of 6.0 mM at pH 7.60 (Martell & Smith, 1974). The EGTA was needed to sequester the 0.025 mol % rated content of Ca in the MgCl₂, so that free Ca²⁺ should have remained less than 10⁻⁸[Mg²⁺] throughout.

Fluorescence spectra were recorded on a Perkin-Elmer MPF-44 spectrofluorometer in the energy mode with a 5-nm bandwidth on excitation and a 10-nm bandwidth on emission. No attempt was made to deaerate solutions. Excitation spectra were corrected by means of a Rhodamine B quantum counter.

Correction factors for the emission monochromator and photomultiplier were obtained by comparing the emission spectra of reference compounds with their known quantum distributions (Lippert et al., 1959). The quantum yield was determined by comparison with a reference solution of quinine bisulfate having the same absorbance as the sample at the exciting wavelength (Pesce et al., 1971); these absorbances were kept below 0.1.

Binding to membranes was assessed by adding well-washed packed human red cells to 100 μ M solutions of BAPTA in media containing 75 mM NaCl, 75 mM KCl, 10 mM Tris at pH 8, and either 100 μ M Tris-EGTA or 1 mM CaCl₂. The final hematocrit was about 18%. After a 1-min equilibration, the suspension was centrifuged and the absorbance of the supernatant measured at 237, 254, 290, and 411 nm on a Zeiss PMQII spectrophotometer. These absorbances were corrected for traces of cell lysis by comparison with spectra of cell supernatants without BAPTA. The difference between BAPTA absorbances before and after the addition and centrifugation of cells was taken to indicate binding to the cells.

Microinjections of BAPTA into giant muscle fibers from the barnacle *Balanus nubilus* were made by a procedure similar to that of Brinley (1968). Microinjections of BAPTA into embryos of the toad *Xenopus laevis* were made following the method of Baker & Warner (1972).

Results

BAPTA: H⁺ Binding. The first two ionizations of BAPTA are below pH 4 and cannot be determined accurately since BAPTA is rather insoluble as an uncharged or singly ionized species. The highest two pK_as are 6.36 and 5.47, measured in 0.1 M KCl. The uncertainty of these pK_as is calculated to be ±0.1, based on the residual sum of squares in the least-squares fit.

UV Spectra and Metal Binding. UV absorption spectra of BAPTA at various levels of free Ca²⁺ are shown in Figure 1. In the absence of Ca²⁺, the spectrum shows a maximum at 254 nm (ϵ 1.6 × 10⁴ M⁻¹ cm⁻¹) with a shoulder at 287 nm (ϵ 5.6 × 10³). There is also a short wavelength maximum at 209 nm (ϵ 3.8 × 10⁴) not shown in Figure 1. As predicted, the spectrum of uncomplexed BAPTA resembles that of a dialkylaniline or anisidine (Klevens & Platt, 1949). Ca²⁺ binding causes a major hypsochromic shift toward a limiting spectrum having a small maximum at 274 nm (ϵ 4.2 × 10³) and the main peak at 203 nm (ϵ 4.1 × 10⁴). This spectrum is much closer to that of an alkylbenzene or anisole (Dearden & Forbes, 1959). Curves intermediate between these two extremes are obtained in Ca²⁺-EGTA buffers in which the BAPTA at 100 μ M responds to but cannot significantly perturb the Ca²⁺ level set by the 10 mM EGTA. Such a series of spectra is conveniently analyzed by a Hill plot, i.e., a plot of log [(A - A₀)/(A₁ - A)] ≡ y vs. log [Ca²⁺] ≡ x. A₀ is the absorbance of the free tetraanion, A₁ the absorbance of the Ca²⁺ complex, and A the absorbance at an intermediate Ca²⁺ level, all measured at the same wavelength. The Hill plots for 254 and 290 nm give a single straight line with slope = 1 from y = -1 to +1 (9–91% saturation), indicating that the stoichiometry is simply 1 Ca²⁺/1 BAPTA. The x intercept indicates the dissociation constant of the complex to be 107 nM. A further check on the stoichiometry is to vary the BAPTA concentration from 10 μ M to 1 mM in solutions with well-buffered Ca²⁺. Similar experiments were responsible for proving that arsenazo III formed complexes with 1 Ca²⁺/2 dyes (Thomas, 1979). However, the spectrum of BAPTA always has the same shape for a given Ca²⁺ level, be it <1 nM, 100 nM (half-saturation), or 1 mM (full saturation), confirming that the complex con-

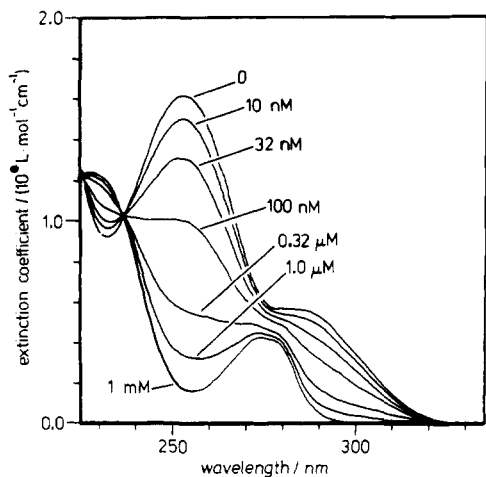


FIGURE 1: Absorption spectrum of BAPTA as a function of free Ca^{2+} concentration. $[\text{Ca}^{2+}]$ was set by EGTA buffers with compositions as follows: $[\text{Ca}^{2+}] = 0$, 10 mM $\text{K}_2\text{H}_2\text{EGTA}$; $[\text{Ca}^{2+}] = 10$ nM, 0.909 mM $\text{K}_2\text{CaEGTA} + 9.09$ mM $\text{K}_2\text{H}_2\text{EGTA}$; $[\text{Ca}^{2+}] = 32$ nM, 2.4 mM $\text{K}_2\text{CaEGTA} + 7.6$ mM $\text{K}_2\text{H}_2\text{EGTA}$; $[\text{Ca}^{2+}] = 100$ nM, 5.0 mM $\text{K}_2\text{CaEGTA} + 5.0$ mM $\text{K}_2\text{H}_2\text{EGTA}$; $[\text{Ca}^{2+}] = 0.32$ μM , 7.6 mM $\text{K}_2\text{CaEGTA} + 2.4$ mM $\text{K}_2\text{H}_2\text{EGTA}$; $[\text{Ca}^{2+}] = 1.0$ μM , 9.09 mM $\text{K}_2\text{CaEGTA} + 0.909$ mM $\text{K}_2\text{H}_2\text{EGTA}$; $[\text{Ca}^{2+}] = 1$ mM, 1 mM CaCl_2 . All solutions contained 100 μM K_4BAPTA , 100 mM KCl , and 10 mM Mops and were titrated to pH 7.29 with KOH . The reference cuvette was filled with the same buffer solution without the BAPTA. The stock solution of K_2CaEGTA was prepared by titration of $\text{K}_2\text{H}_2\text{EGTA}$ with CaCl_2 to the potentiometric end point measured by a Ca^{2+} -selective electrode (Ammann et al., 1975). This procedure achieves a more accurate equality of Ca and EGTA contents than simply weighing out the constituents and hoping that their purities are the same.

tains just 1 BAPTA. Simple 1:1 stoichiometry was of course to be expected by analogy to EGTA and contrasts with 0–3 effective Ca^{2+} per 1 aequorin and 1 Ca^{2+} per 2 arsenazo III molecules.

BAPTA has much less affinity for Mg^{2+} than for Ca^{2+} , as predicted. Figure 2a shows the effect of Mg^{2+} on the absorbance of BAPTA, from which a dissociation constant of Mg^{2+} –BAPTA of 17 mM can be deduced (Figure 2b). This binding is about 5.2 log units weaker than the binding of Ca^{2+} . The spectral shift corresponding to the 17 mM estimate is only about half that produced by Ca^{2+} binding; the remaining half requires much higher Mg^{2+} concentrations, hundreds of mM. The interpretation is obvious. The first Mg^{2+} ion binds primarily to just one of the two halves of BAPTA and does not perturb the spectrum of the other aromatic nucleus. Above 100 mM Mg^{2+} a second Mg^{2+} begins to bind to the previously unperturbed half of the ligand and completes the spectral change. The dissociation constant for the second binding, ~ 0.5 M, is not quantitatively comparable to the first, since they are measured at different ionic strengths. The finding that one Mg^{2+} ion affects only half of BAPTA, whereas one Ca^{2+} ion affects both halves, is a striking confirmation of the design of the binding cavity, a good fit for Ca^{2+} but too big to hold Mg^{2+} snugly.

The effect of pH on the UV spectrum confirms the titration pK_a s. Increasing acidity has very little effect on the spectrum until the pH drops below 6.5 or so. Once protons are taken up, they produce much the same effect on the spectrum as Ca^{2+} or Mg^{2+} does. Protonation of an amino substituent is well-known to destroy the conjugation of the nitrogen with the ring; the great spectral similarity between proton and metal additions supports the belief that metal binding does indeed destroy the chromophore conjugation as designed. This behavior is the reverse of the previously known metallochromic

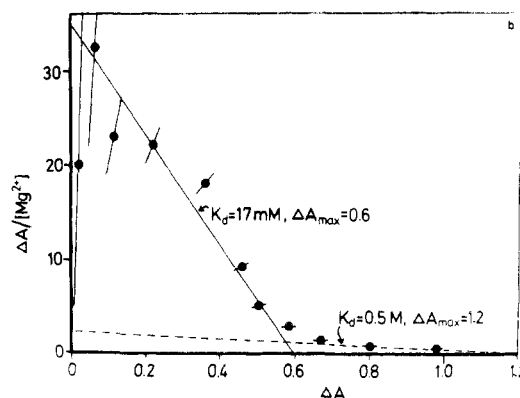
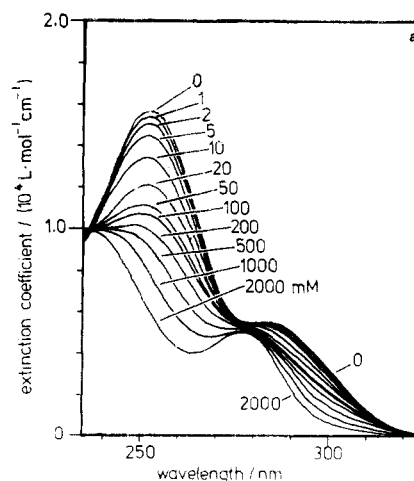


FIGURE 2: (a) Absorption spectrum of BAPTA as a function of free Mg^{2+} concentrations, set by buffers with compositions as follows ($[\text{Mg}^{2+}]$, MgCl_2 , $\text{K}_2\text{H}_2\text{EGTA}$, KCl , all in mM): 0, 0, 2, 100; 1, 1.33, 2.33, 96; 2, 2.67, 2.67, 92; 5, 6.67, 3.67, 80; 10, 13.33, 5.33, 60.5; 20, 26.67, 8.67, 21; 50, 66.7, 18.7, 0; 100, 116.7, 17.7, 0; 200, 233, 34, 0; 500, 583, 84, 0; 1000, 1167, 168, 0; 2000, 2333, 334, 0. All solutions also contained 100 μM K_4BAPTA and 10 mM Hepes and were titrated to pH 7.60 with KOH . Solutions with $[\text{Mg}^{2+}] = 0$ –50 mM are calculated to have 2 mM free $\text{H}_2\text{EGTA}^{2-}$; solutions with $[\text{Mg}^{2+}] = 100$ –2000 mM should have 1 mM free $\text{H}_2\text{EGTA}^{2-}$. Up to $[\text{Mg}^{2+}] = 20$ mM, the total ionic strength is held approximately constant at 111 mM by adjustment of the KCl addition, but at higher $[\text{Mg}^{2+}]$ the ionic strength rises sharply. (b) Scatchard-type plot of the absorbances from Figure 2a, measured at 253 nm. ΔA is the difference between the absorbance A_0 at $[\text{Mg}^{2+}] = 0$ and the absorbance A at some $[\text{Mg}^{2+}]$ between 1 and 2000 mM inclusive. ΔA is expected to be proportional to the average number of Mg^{2+} ions bound per BAPTA. The error bars show the calculated effect on ΔA and $\Delta A/[\text{Mg}^{2+}]$ of uncorrelated variations of $\pm 1\%$ in the BAPTA concentration from solution to solution. The solid and broken lines are the theoretical plots for the equations $\Delta A = 0.6[\text{Mg}^{2+}/17 \text{ mM}]/(1 + [\text{Mg}^{2+}/17 \text{ mM}])$ and $\Delta A = 1.2[\text{Mg}^{2+}/0.5 \text{ M}]/(1 + [\text{Mg}^{2+}/0.5 \text{ M}])$, respectively.

Ca^{2+} indicators, in which Ca^{2+} gain has roughly the same spectral appearance as proton loss.

Large variations in sodium and potassium concentrations cause only slight shifts of the absorption spectrum (Figure 3). Clearly the alkali metal cations are unable to disrupt the conjugation of the nitrogen lone-pair electrons with the ring.

Fluorescence. The fluorescence emission spectrum of BAPTA shows a peak at 363 nm with no fine structure; the quantum efficiency was found to be 0.027. Binding of Ca^{2+} reduces the emission intensity by a factor of 2.8 without significantly altering the shape of the band or the wavelength of its peak. The corrected excitation spectra agreed reasonably well with the absorbance spectra.

NMR Spectra and Kinetics of Ca^{2+} Binding. The proton magnetic resonance spectrum of K_4BAPTA in D_2O shows the

Table I: Ca^{2+} and Mg^{2+} Affinities and UV Absorption Peaks of New Ligands

structure	log stability constants ^a		absorption maxima ^b		isosbestic points ^b	peaks of difference spectrum ^{b,c}
	Ca^{2+}	Mg^{2+}	free anion	Ca^{2+} complex		
2a	6.97	1.77	254 (16), 287 (5.6)	274 (4.2)	237 (10)	254 (14.5), 290 (4.9)
2b	7.4	d	251 (13), 282 (4.6)	279 (4.9)	275 (4.7), 284 (4.6)	255 (10), 295 (2.6)
2c	5.8	<1	263 (20)	240 (16), 282 (5.2)	247 (14)	264 (16), 299 (5.7)
3a	7.6	3.0	262 (34), 350 (4.1)	233 (36), 279 (6.2), 316 (3.8)	240 (19), 290 (5.3), 315 (3.8), 318 (3.3)	271 (30), 360 (3.4)
3b	7.1	2.7	261 (37), 354 (5.0)	240 (36), 332 (5.0)	248 (31), 319 (4.2), 339 (4.6)	265 (29), 365 (4.1)
4	6.9	4.3	270 (19)	271 (7)	none above 230 nm	271 (12)
5	5.5	1.8	256 (19), 293 (6.4)	275 (5.6), 280 (5.6)	280 (5.6)	255 (18), 296 (6)
6	4.1	3.0	257 (19), 350 (3.2)	231 (22), 301 (4)	240 (12), 275 (2.6), 319 (2.2)	257 (14), 295 (-2.6), 350 (2.7)

^a Defined as $\log [\text{ML}]/([\text{M}][\text{L}])$, where $[\text{M}]$, $[\text{L}]$, and $[\text{ML}]$ are the concentrations of free metal, ligand, and complex, respectively, expressed as mol/L, in 0.1 M KCl, at $22 \pm 2^\circ\text{C}$. ^b The first number is the wavelength in nm; in parentheses is the corresponding extinction coefficient ϵ or $\Delta\epsilon$ in units of $10^3 \text{ L mol}^{-1} \text{ cm}^{-1}$. ^c A positive $\Delta\epsilon$ means that the free anion exceeds the Ca^{2+} complex in absorbance. ^d Not measured.

aromatic protons in a complex pattern at τ 2.9–3.1, the ethane bridge at τ 5.64, and the acetate protons at τ 6.29, with the integrals in the expected ratio of 8:4:8. Addition of excess Ca^{2+} shifts the aromatic peaks downfield by 0.2 ppm, the ethane bridge protons downfield by 0.15 ppm, but the acetate protons slightly upfield. When only 0.5 mol of Ca^{2+} per mol BAPTA has been added, each of the three main peaks remains coalesced and has a chemical shift intermediate between its zero- Ca^{2+} and full- Ca^{2+} values. This demonstrates that each individual molecule of BAPTA takes up and unloads Ca^{2+} at a rapid rate. A rough lower bound to the exchange rate is $\pi\Delta\nu$, where $\Delta\nu$ is the chemical shift difference between the zero- Ca^{2+} and full- Ca^{2+} signals (Pople et al., 1959). Substituting $\Delta\nu = 0.2 \text{ ppm} \times 100 \text{ MHz} = 20 \text{ Hz}$, the rate constant for exchange must be at least 60 s^{-1} . If the exchange rate were slower than this, one would have observed each of the three main peaks to split into a pair of peaks, the new member of which would grow at the expense of the old as Ca^{2+} ions were progressively added. EGTA shows precisely this latter sort of behavior (Bryson & Nancollas, 1965), confirmed in this study under conditions similar to those of the BAPTA experiment, showing that it is very much slower at exchanging Ca^{2+} ions.

Biological Tests. Binding of BAPTA to human erythrocyte membranes is too weak to be reliably measured. At 18% hematocrit, less than 8% of the total BAPTA or Ca^{2+} -BAPTA at 100 μM concentration is bound to the cells. The amount bound to a membrane surface is therefore less than that contained in a layer 0.3 μm thick of adjacent aqueous solution.

Preliminary tests have been made for intracellular effects. BAPTA was microinjected into muscle fibers from the barnacle *B. nubilus* to a final concentration of several mM. Muscle contraction was abolished as expected for a potent Ca^{2+} buffer. The inhibition could be reversed by the further injection of an equivalent quantity of Ca^{2+} , showing that there were no gross toxic effects on the contractile or metabolic systems. ^{22}Na effluxes were monitored in one fiber and showed no significant change. (C. C. Ashley, T. J. Rink, and R. Y. Tsien, unpublished experiments.)

Microinjection of Ca^{2+} -BAPTA buffers into early embryos of *X. laevis* to a final buffer concentration of $\sim 10 \text{ mM}$ caused effects qualitatively similar to those of Ca^{2+} -EGTA injections (Baker & Warner, 1972) in that a few eggs failed to divide and the remainder were slowed. At half-saturation of the BAPTA (Ca^{2+} near 10^{-7} M), 70% of the eggs continued development (Rink et al., 1980). No developmental deformities were seen in specimens kept to a late tadpole stage.

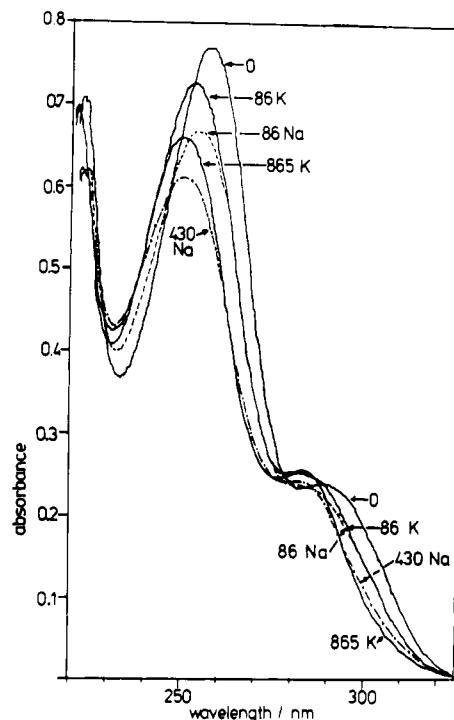
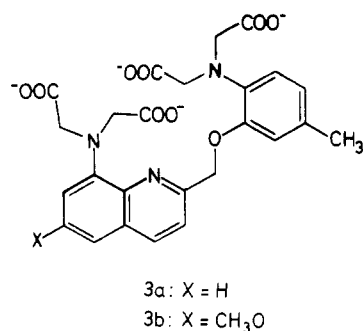


FIGURE 3: Absorbance spectra of BAPTA (50 μM) in solutions with various concentrations of K^+ and Na^+ . All solutions contained 20 mM Me_4N^+ , 10 mM EGTA, and 10 mM Mops, titrated to pH 7.4, plus the indicated concentrations of KCl or NaCl in mM; an exception was the curve labeled 0, which had 106.5 mM total Me_4N^+ and 86.5 mM Cl^- .

Simple Derivatives (2b,c) of BAPTA. Cation affinities in the BAPTA family can be tuned up or down by appropriate electron-donating or -withdrawing substituents. Table I summarizes the affinities for Ca^{2+} and Mg^{2+} deduced from UV absorption spectra as described above for BAPTA. Thus substitution of methyl groups for hydrogens to give structure 2b strengthens Ca^{2+} binding by 0.4 log unit; substitution of bromine atoms for the same hydrogens to give 2c weakens Ca^{2+} binding by 1.2 log units to a dissociation constant of 1.7 μM . H^+ and Mg^{2+} uptake are also weakened to the point where they can be disregarded for practically all biological applications (highest $\text{pK}_a = \sim 5.6$; dissociation constant of Mg^{2+} complex $> 100 \text{ mM}$).

Quinolines 3a,b. Further adjustments of the Ca^{2+} and Mg^{2+} affinities (Table I) result from modification of the ether linkage between the aromatic nuclei. In 3a and 3b, one of the ether oxygens of BAPTA (2a) has been replaced by an sp^2 -



hybridized heterocyclic nitrogen. Since such nitrogen atoms are considerably more basic than ether oxygens, it is not surprising that **3a** has significantly higher affinity for both Ca²⁺ and Mg²⁺ than BAPTA (**2a**). The increase in the size of the chromophore shifts the wavelengths of absorption and fluorescence to 350 and 520 nm. The free anion of **3a** has a quantum yield of ~0.012; binding of Ca²⁺ causes a very slight red shift and a large increase in quantum efficiency to ~0.057. Mg²⁺ causes the same slight red shift but a much smaller increase in quantum efficiency, to ~0.015.

Compounds **3a** and **3b** differ only by one methoxy group. Since the methoxy group is meta to the 8-amino group, it should exert an electron-withdrawing effect and indeed lowers both Ca²⁺ and Mg²⁺ affinities by ~0.3–0.5 log unit. The UV spectra of ligand **3b** and its complexes are shown in Figure 4. As usual, complexation causes a profound shift in the absorption spectrum, as if the 8-amino substituent were disconnected from the rest of the chromophore. Notice that the two complexes do not have the same spectrum. The difference between the Mg²⁺ and Ca²⁺ spectra is quantitatively explained if the right-hand benzene ring system participates in the chelation of Ca²⁺ but not of Mg²⁺. The predicted spectroscopic effect of engaging the right-hand nucleus in chelation is just half the difference between BAPTA and Ca–BAPTA spectra and fits well the observed difference between Mg²⁺ and Ca²⁺ spectra of compound **3b**.

The methoxy group in **3b** has a useful role in enhancing the quantum yield of fluorescence. The free anion of **3b** has an emission maximum at 510 nm and a quantum yield of ~0.029, some 2.5 times higher than the quinoline without the methoxy group. Ca²⁺ binding again causes a very slight shift of the emission to ~525 nm and a fivefold enhancement of the quantum yield to ~0.14. The effect of Mg²⁺ is now the opposite, a 25% decrement in emission amplitude.

Further Derivatives. Ligands **4** and **5** serve to demonstrate that more drastic changes in the number and geometrical disposition of chelating groups destroy the high Ca²⁺/Mg²⁺ specificity of the previous compounds. In ligand **4**, the two weakly liganding ether oxygens of BAPTA have been replaced by >NCH₂COO⁻ groups providing four much stronger ligand groups. The Ca²⁺ affinity changes negligibly but the Mg²⁺ affinity increases 350-fold. In ligand **5**, one ether oxygen has been incorporated into a five-membered ring whose bond angles should keep the nitrogens further apart and make the binding site less compact than BAPTA; now Mg²⁺ affinity is unaffected while Ca²⁺ affinity falls by 1.5 log units.

Solubility and Stability. Aqueous solubilities of the new ligands have not been quantified, but in general the potassium salts of the ligands and their Ca²⁺ complexes are soluble to at least several hundred mM. Solutions of the tetraanions exposed to air slowly darken, becoming faintly brown after 1 month or so at room temperature. This process is probably aerial oxidation, a common reaction for aromatic amines. Storage either as a dry solid, frozen solution, or Ca²⁺ complex

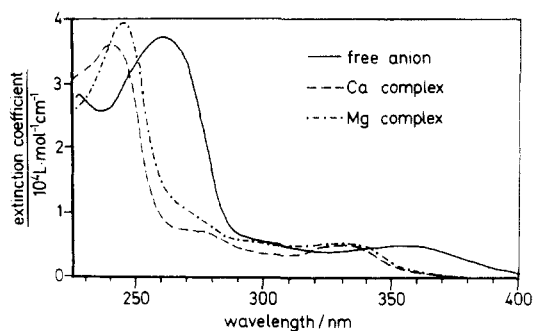


FIGURE 4: Absorption spectra of the methoxyquinoline ligand **3b** and its Ca²⁺ and Mg²⁺ complexes, all at 5×10^{-5} M. The free tetraanion was measured in 0.1 M KCl + 5 mM K₂H₂EGTA, the Mg²⁺ complex in the same medium plus 100 mM MgCl₂, and the Ca²⁺ complex in 0.1 M KCl and 1 mM CaCl₂. All pHs were between 7.4 and 7.7.

in solution greatly hinders darkening. Derivatives with substituents para to the amino groups also seem less susceptible to oxidation.

Discussion

The present indicator design aims at a much higher Ca²⁺ affinity than previous indicators such as aequorin, arsenazo III, or murexide, so that a sizable but not overwhelming proportion of indicator molecules become complexed with Ca²⁺. However, it has been argued (Scarpa et al., 1978a,b; Brinley, 1978) that such high affinity is undesirable because absorbance increments at any given wavelength are no longer directly proportional to [Ca²⁺] and because the indicator may become a significant load on the intracellular Ca²⁺-buffering capacity. But there are counterarguments favoring an indicator whose Ca²⁺ dissociation constant is comparable to the level of Ca²⁺ being measured, typically $10^{-7.5}$ – 10^{-5} M. These are analogous to the reasons why pH values near 7 are measured with indicators with pK_as near 7 (Chance & Scarpa, 1972) rather than 4 or 5. If the indicator is near 50% saturation, the shape of its spectrum is a sensitive measure of the ratio of bound to free indicator. This ratio is directly proportional to the ion concentration sought, independent of total indicator dosage or optical path length. By contrast, an indicator which is <1% saturated is very insensitive to the static value of [Ca²⁺]. It does give tiny but detectable absorbance increments linearly related to [Ca²⁺] changes. Unfortunately, the constant of proportionality depends on indicator dosage and cell thickness, which are frequently not well-defined. Thus both resting levels and transient amplitudes are hard to calibrate.

The second advantage of high Ca²⁺ affinity is that a much smaller total amount of dye needs to be infiltrated into the cell for a given optical sensitivity. Suppose, for example, that high- and low-affinity indicators undergo the same change in their molecular extinction coefficients when a Ca²⁺ ion binds. To give the same final absorbance change, either dye would therefore have to bind the same absolute number of Ca²⁺ ions, imposing the same buffering load on the cell, but the low-affinity dye would also need a huge excess of free dye to drive the complexation reaction to the stipulated extent. Obviously the less the total amount of dye that has to be introduced the easier its intracellular administration and the less danger of toxic side effects. A high-affinity indicator need not perturb the preexisting Ca²⁺ level any more than a low-affinity indicator, since so much less dye is needed.

Though the Ca²⁺ affinity of BAPTA is reasonably well matched to the resting Ca²⁺ levels typical inside many cells ($\sim 10^{-7}$ M), BAPTA itself is useless as an intracellular indicator because its absorption peaks are at too short a wave-

length, directly underneath the absorption of aromatic amino acids and nucleic acids. It was prepared as a model compound in which the long-wavelength absorption of an extended chromophore was deliberately sacrificed to make the synthesis as short as possible and allow a quick test of the basic design principles. It still could find application simply as a high-quality Ca^{2+} buffer if it became commercially available. As a Ca^{2+} buffer it has three advantages over EGTA: insensitivity of effective Ca^{2+} affinity to pH; speed of buffering, particularly important when trying to show that some transient physiological response can be suppressed by excess buffer (Hellam & Podolsky, 1969); the ability directly to check the Ca^{2+} level of the buffer by UV spectroscopy. By contrast, the Ca^{2+} level of a Ca^{2+} -EGTA buffer is known only by a complicated dead-reckoning procedure from the pH, total Ca^{2+} , Mg^{2+} , and EGTA initially added.

Further advances should be realizable by the synthesis of other derivatives of BAPTA. The effect of substituents on the cation affinities should be quantitatively predictable by a Hammett-type linear free-energy relation. Such a variation of substituents should give a whole series of related buffers of graded Ca^{2+} affinities while maintaining good ionic selectivity. One could then choose the buffer whose dissociation constant best matched the desired buffering level, rather than be forced to use EGTA even where it has a very poor buffering capacity. The advantage may be appreciated by imagining how inconvenient it would be to have only one pH buffer, say tris(hydroxymethyl)aminomethane, to cover all pHs from 6 to 9 (Good & Izawa, 1972).

Compared with BAPTA, quinolines **3a** and **3b** offer much longer wavelengths of absorption and fluorescence and higher emission quantum yields. Their optical properties are roughly similar to dansyl groups in aqueous media (Seiler, 1970). However, they are more tedious than BAPTA to synthesize, and they have somewhat less $\text{Ca}^{2+}/\text{Mg}^{2+}$ selectivity, in accord with the suggestion (Williams, 1970) that nitrogen donors intrinsically show more preference than oxygen for Mg^{2+} over Ca^{2+} . Nevertheless their selectivity of $>2 \times 10^4$ is still better than that of any previous metallochromic dyes. It is instructive to compare quinoline **3a** with its isolated halves as represented by (*o*-methoxyphenyl)iminodiacetic acid and compound **6**, 8-[bis(carboxymethyl)amino]quinoline. The Ca^{2+} affinity of ligand **3a** exceeds that of quinoline **6** by 3.5 log units. The added (alkoxyphenyl)iminodiacetate would have a log stability constant for Ca^{2+} of about 2.9 by itself, based on 2.75 for (*o*-methoxyphenyl)iminodiacetate (Irving & da Silva, 1963), plus a small correction due to the methyl substituent. Therefore a Ca^{2+} bound to half of quinoline **2** is presented to the other half with an effective concentration (Jencks, 1975) of 4 M. By contrast, the Mg^{2+} affinities of **3a** and **6** are practically the same, confirming the spectroscopic evidence that the (alkoxyphenyl)iminodiacetate moiety does not participate in the binding of Mg^{2+} . Presumably this is because it cannot approach closely enough to complete a sufficiently compact binding site.

In ligand **3b** the methoxy group was placed at the 6 position in the hope that the Ca^{2+} complex would fluoresce like the 6-methoxyquinolinium fluorophore responsible for the strong fluorescence of the quinine cation. The methoxy group did increase the quantum yield over that of quinoline **3a**, but not to the 0.55 of quinine (Pesce et al., 1971). Also, the longer peak wavelength of emission (525 nm vs. 440–460 nm for quinine) suggests that, despite the Ca^{2+} ion, the 8-amino group may still be exerting a bathochromic influence on the emission of the complex. Why Mg^{2+} should cause a diminution of

quantum yield, and a slight one at that, is unclear.

Derivatives of BAPTA (**2a**) and the quinolines **3a,b** with yet longer conjugated chromophores have been prepared and are visibly absorbing and fluorescing indicators to be described in later papers.

Acknowledgments

I thank Dr. T. J. Rink for helpful discussion, Drs. C. Ashley and A. Warner for collaboration on the microinjection experiments, and the Cambridge University Chemical Laboratory for providing facilities for organic synthesis and NMR spectroscopy.

References

- Ammann, D., Gueggi, M., Pretsch, E., & Simon, W. (1975) *Anal. Lett.* **8**, 709–720.
- Ashley, C. C., & Campbell, A. K., Eds. (1979) *Detection and Measurement of Free Calcium Ions in Cells*, Elsevier, Amsterdam.
- Baker, P. F., & Warner, A. E. (1972) *J. Cell Biol.* **53**, 579–581.
- Beck, M. T. (1970) *The Chemistry of Complex Equilibria* (Chalmers, R. A., Transl.) pp 132–133, Chapman and Hall, London.
- Blinks, J. R., Prendergast, F. G., & Allen, D. G. (1976) *Pharmacol. Rev.* **28**, 1–93.
- Blinks, J. R., Mattingly, P. H., Jewell, B. R., van Leeuwen, M., Harrer, G. C., & Allen, D. G. (1978) *Methods Enzymol.* **57**, 292–328.
- Brinley, F. J., Jr. (1968) *J. Gen. Physiol.* **51**, 445–477.
- Brinley, F. J., Jr. (1978) *Annu. Rev. Biophys. Bioeng.* **7**, 363–392.
- Brown, J. E., Brown, P. K., & Pinto, L. H. (1977) *J. Physiol. (London)* **267**, 299–320.
- Bryson, A., & Nancollas, G. H. (1965) *Chem. Ind. (London)*, 655.
- Chance, B., & Scarpa, A. (1972) *Methods Enzymol.* **24**, 336–342.
- Claisen, L., & Eisleb, O. (1913) *Justus Liebigs Ann. Chem.* **401**, 21–119.
- Dearden, J. C., & Forbes, W. P. (1959) *Can. J. Chem.* **37**, 1305–1314.
- Duncan, C., Ed. (1976) *Symp. Soc. Exp. Biol.* **30**, 1–485.
- Good, N. E., & Izawa, S. (1972) *Methods Enzymol.* **24**, 53–68.
- Hellam, D. C., & Podolsky, R. J. (1969) *J. Physiol. (London)* **200**, 807.
- Irving, H., & da Silva, J. J. R. F. (1963) *J. Chem. Soc.*, 3308–3320.
- Jaunin, R., & Holl, R. J. (1958) *Helv. Chim. Acta* **41**, 1783–1792.
- Jencks, W. P. (1975) *Methods Enzymol.* **43**, 219–410.
- Klevens, H. B., & Platt, J. R. (1949) *J. Am. Chem. Soc.* **71**, 1714–1720.
- Kretsinger, R. H., & Nelson, D. J. (1976) *Coord. Chem. Rev.* **18**, 29–124.
- Lippert, E., Naegel, W., Seibold-Blankenstein, I., Staiger, U., & Voss, W. (1959) *Fresenius' Z. Anal. Chem.* **170**, 1–18.
- Madeja, K. (1962) *J. Prakt. Chem.* **17** (4), 97–103.
- Martell, A. E., & Smith, R. M. (1974) *Critical Stability Constants*, Vol. 1, Plenum Press, New York.
- Mathur, F. C., & Robinson, R. (1934) *J. Chem. Soc.*, 1520–1523.
- Moiescu, D. G., Ashley, C. C., & Campbell, A. K. (1975) *Biochim. Biophys. Acta* **396**, 133–140.

- Pesce, A. J., Rosen, C.-G., & Pasby, T. L. (1971) *Fluorescence Spectroscopy*, pp 177-178, Marcel Dekker, New York.
- Pople, J. A., Schneider, W. G., & Bernstein, H. J. (1959) *High Resolution Nuclear Magnetic Resonance*, pp 222-223, McGraw-Hill, New York.
- Rink, T. J., Tsien, R. Y., & Warner, A. E. (1980) *Nature (London)* 283, 658-660.
- Scarpa, A., & Carafoli, E., Eds. (1978) *Ann. N.Y. Acad. Sci.* 307, 1-655.
- Scarpa, A., Brinley, F. J., Jr., & Dubyak, G. (1978a) *Biochemistry* 17, 1378-1386.
- Scarpa, A., Brinley, F. J., Jr., Tiffert, T., & Dubyak, G. (1978b) *Ann. N.Y. Acad. Sci.* 307, 545-561.
- Seiler, N. (1970) *Methods Biochem. Anal.* 18, 259-337.
- Tasker, P. A., & Fleischer, E. B. (1970) *J. Am. Chem. Soc.* 92, 7072-7077.
- Thomas, M. V. (1979) *Biophys. J.* 25, 541-548.
- Williams, R. J. P. (1970) *Q. Rev., Chem. Soc.* 24, 331-365.

Further Studies on the Structural Requirements for Synthetic Peptide Chemoattractants[†]

Richard J. Freer,* Alan R. Day, Jeffrey A. Radding, Elliott Schiffmann, S. Aswanikumar, Henry J. Showell, and Elmer L. Becker

ABSTRACT: Thirty small molecular weight peptides related to the chemotactic peptide *N*-formylmethionylleucylphenylalanine (CHO-Met-Leu-Phe-OH) have been prepared by both solid-phase and classical peptide synthesis. Compounds were prepared to investigate the structural requirements in the 1 position (*N*-formylmethionine) and the 3 position (phenylalanine). Each analogue was tested for its ability to induce lysosomal enzyme release from cytochalasin B treated rabbit polymorphonuclear leukocytes in vitro. In addition, some were also tested for their ability to stimulate neutrophil chemotaxis in vitro and for inhibition of specific binding of a ³H-labeled chemotactic peptide, CHO-Nle-Leu-Phe-OH. The results show that the formyl group of CHO-Met-Leu-Phe-OH is essential for good biological activity since *N*-acetylation, removal of the α -amino group (i.e., desamino), or replacement by an ethyl group results in a drastic loss of chemotactic potency (approximately 5000-fold). In addition, the sulfur-

containing side chain of methionine produces optimum activity of the tripeptide. Analogues containing other sulfur amino acids [ethionine, Cys(Me)] were less active, as were a variety of analogues containing linear aliphatic, aromatic, or branched aliphatic side chains at position 1. A limited number of analogues were prepared to probe structure-activity relationships at position 3. The data indicate that the primary sequence, Met-Leu-Phe, generates the most active chemoattractants, although addition of a large, highly charged Lys residue allowed the retention of a large degree of chemotactic activity. A free carboxyl group may be desirable, however, since CHO-Met-Leu- β -phenethylamine (-descarboxy-Phe) is relatively inactive. Finally, several related compounds have been identified which are specific competitive antagonists of CHO-Met-Leu-Phe-OH-induced lysosomal enzyme release and chemotaxis.

Although a large number of partially or totally uncharacterized substances have been reported to be chemotactic for neutrophils (Wilkinson, 1974), a systematic study of the phenomenon at the molecular level was not possible due to the unknown structure of these chemoattractants. In recent years, however, the finding of Schiffmann et al. (1975) that *N*-formylmethionine was chemotactic stimulated the development of a new group of synthetic chemoattractants. These are small molecular weight, *N*-acylated di-, tri-, and tetrapeptides, the most active of which is *N*-formyl-Met-Leu-Phe-OH [ED₅₀ for chemotaxis of (7-9.1) × 10⁻¹¹ M]. These compounds were also shown to induce the release of lysosomal enzymes (Showell et al., 1976), an effect which was absolutely correlated (*R* > 0.95) with their ability to stimulate chemotaxis. In addition, by the use of a radiolabeled analogue (*N*-formyl-Nle-Leu-[³H]Phe-OH) (Day et al., 1977), specific binding sites on both rabbit (Aswanikumar et al., 1977a) and human (Williams et

al., 1977) neutrophils were demonstrated. Later work with rabbit neutrophils has shown that these receptors are in the extracellular membrane and have a dissociation constant (*K*_D = 2.9 × 10⁻⁹ M) for the ³H-labeled chemoattractant virtually identical with the ED₅₀ (6.6 × 10⁻¹⁰ M) for the unlabeled chemoattractant (CHO-Nle-Leu-Phe-OH) (Sha'afi et al., 1978).

It was clear from our earlier studies (Showell et al., 1976) that the receptor substance for this group of peptides exhibited striking specificity. For example, in every instance tested, *N*-formylation of these peptides enhanced chemotactic potency by 1000-20 000-fold. Also, there were marked increases in biological activity in a series of tripeptides when compared to a reference dipeptide, *N*-formyl-Met-Leu-OH. Maximum activity was observed with the acylated tripeptide *N*-formyl-Met-Leu-Phe-OH (ED₅₀ for chemotaxis of 7.0 × 10⁻¹¹ M), although a highly active tetrapeptide, *N*-formyl-(Met)₄-OH (ED₅₀ for chemotaxis of 3 × 10⁻¹⁰ M), was also identified. In addition to the size and *N*-acylation requirements, it was also found that methionine at position 1 and phenylalanine at position 3 optimized activity.

In this study we have further evaluated the structure-activity relationship in the highly active CHO-Met-Leu-Phe-OH. This includes an extensive investigation of the role of the *N*-formylmethionine residue. This has resulted in identification of specific antagonists of CHO-Met-Leu-Phe-OH-induced

[†] From the Department of Pharmacology, Medical College of Virginia, Richmond, Virginia 23298 (R.J.F., A.R.D., and J.A.R.), the Laboratory of Developmental Biology and Anomalies, National Institute of Dental Research, National Institutes of Health, Bethesda, Maryland 20014 (E.S. and S.A.), and the Department of Pathology, University of Connecticut Health Center, Farmington, Connecticut 06032 (H.J.S. and E.L.B.). Received May 31, 1979. This work was supported by National Institute of Dental Research Contract DE-62494 and U.S. Public Health Service Grant AI-09648.